β-Subunit of the voltage-gated Ca^{2+} channel Cav1.2 drives signaling to the nucleus via H-Ras

Evrim Servili[a], Michael Trus[a], Daphne Maayan[a], and Daphne Atlas[a,1]

[a]Department of Biological Chemistry, Hebrew University of Jerusalem, Jerusalem 9190401, Israel

Edited by Joseph Schlessinger, Yale University, New Haven, CT, and approved August 1, 2018 (received for review March 29, 2018)

Depolarization-induced signaling to the nucleus by the L-type voltage-gated calcium channel Cav1.2 is widely assumed to proceed by elevating intracellular calcium. The apparent lack of quantitative correlation between Ca^{2+} influx and gene activation suggests an alternative activation pathway. Here, we demonstrate that membrane depolarization of HEK293 cells transfected with $\alpha_1$1.2/β2b/α2δ subunits (Cav1.2) triggers c-Fos and MeCP2 activation via the Ras/ERK/CREB pathway. Nuclear signaling is lost either by absence of the intracellular β2 subunit or by transfecting the cells with the channel mutant $\alpha_1 1.2^{W440A}$/β2b/α2δ, a mutation that disrupts the interaction between $\alpha_1$1.2 and β2 subunits. Pulldown assays in neuronal SH-SY5Y cells and in vitro binding of recombinant H-Ras and β2 confirmed the importance of the intracellular β2 subunit for depolarization-induced gene activation. Using a Ca^{2+}-impermeable mutant channel $\alpha_1 1.2^{L745P}$/β2b/α2δ or disrupting Ca^{2+}/calmodulin binding to the channel using the channel mutant $\alpha_1 1.2^{I1624A}$/β2b/α2δ, we demonstrate that depolarization-induced c-Fos and MeCP2 activation does not depend on Ca^{2+} transport by the channel. Thus, in contrast to the paradigm that elevated intracellular Ca^{2+} drives nuclear signaling, we show that Cav1.2-triggered c-Fos or MeCP2 is dependent on extracellular Ca^{2+} and Ca^{2+} occupancy of the open channel pore, but is Ca^{2+}-influx independent. An indispensable β-subunit interaction with H-Ras, which is triggered by conformational changes at $\alpha_1$1.2 independently of Ca^{2+} flux, brings to light a master regulatory role of β2 in transcriptional activation via the ERK/CREB pathway. This mode of H-Ras activation could have broad implications for understanding the coupling of membrane depolarization to the rapid induction of gene transcription.

excitation-transcription coupling | Cav1.2 | H-Ras | MeCp2 | c-Fos

Activation of voltage-gated calcium channels (VGCCs) during membrane depolarization induces gene expression in neuronal and muscle cells in a process called excitation-transcription (ET) coupling. In particular, Cav1.2, a member of the L-type Cav1 channels, has been shown to activate a large number of different neuronal-specific genes as well as the classic Fos and Jun immediate-early genes (1–5).

Mechanisms that regulate Cav1.2 activity-dependent transcription of Fos are attributed to a transient increase in intracellular calcium {$[Ca^{2+}]_i$}, mainly through Ca^{2+} activation of calmodulin (CaM) (Ca^{2+}-CaM) (6). They include Ca^{2+}-CaM activation of local cytosolic pools of kinases such as CaMKII (5), Ca^{2+}-CaM binding to the isoleucine-glutamic acid motif (IQ) at the COOH terminus of Cav1.2 (7, 8), and nuclear translocation of Ca^{2+}-CaM, activating the nuclear protein kinase Ca^{2+}-calmodulin kinase IV (CaMKIV) (9). Other proposed pathways involve the calcium-regulated phosphatase calcineurin (9–12) and the activation of the Ras/mitogen-activated protein kinase (MAPK) signaling pathways (8, 13–15). More recent studies have shown that Cav1.2 acts locally with β-calmodulin (CaM) kinase II (βCaMKII) and calcineurin, while γCaMKII acts as a carrier for transporting Ca^{2+}/CaM from the surface membrane to the nucleus and activates CaMKK and CREB kinase (16).

Although the primary role of Cav1 channels is to conduct Ca^{2+} into the cells, depolarization-induced conformational changes in Cav1.2 trigger excitation-secretion (ES) coupling in excitable cells (17–20), or excitation-contraction (EC) coupling in neonate cardiac myocytes (21), independently of Ca^{2+} influx. These studies highlight a metabotropic role of Cav1.2, which similar to membrane receptor, is activated by Ca^{2+} that binds as a selective ligand at the channel pore. It was proposed that membrane depolarization elicits transition from a closed-single Ca^{2+}-occupied pore to the open-double Ca^{2+}-occupied pore, transducing signaling before Ca^{2+} entry. A direct functional and physical interactions of the II–III linker of the $\alpha_1$1.2 subunit with the exocytotic machinery or with RyR2 were shown to trigger ES coupling, or EC coupling, respectively (reviews in refs. 22–24). The Ca^{2+} sensitivity of this conformational-coupled signaling is imparted by the obligatory Ca^{2+} double occupancy of the channel pore, which depends on voltage and extracellular Ca^{2+} concentrations.

ET coupling induced by Cav1.2 is highly effective in cultured cortical neurons and in superior cervical ganglion cells. Despite the relatively minor contribution to synaptic calcium transients, Cav1.2 appears to dominate transcriptional events in cortical neurons of mature cultures (2) (review in ref. 25). This apparent lack of correlation between gene activation and Ca^{2+} influx have led to proposing that signaling by Ca_V1 is mediated through elevated Ca^{2+} at the mouth of the channel (24, 25). Earlier studies have shown that local Ca^{2+} signals are conveyed from the aperture of Cav1.2 to the nucleus via the Ras/MAPK pathway (8, 13, 14) It was also suggested that Ca^{2+} entry and subsequent binding to calmodulin might be responsible for gene activation through Ras (8).

For better understanding the role of Ca^{2+} in depolarization-triggered gene activation, we examined Cav1.2-mediated ET coupling via the ERK/CREB pathway.

Significance

The L-type voltage-gated calcium channel Cav1.2 mediates depolarization-triggered signaling cascades that regulate neuronal-specific transcription factors such as CREB and immediate-early genes. We demonstrate that the interaction of the intracellular β-subunit of the channel with H-Ras is indispensable for depolarization-triggered gene activation. The binding of the recombinant β-subunit to H-Ras and H-Ras pulldown assays confirms the ability of H-Ras to physically interact with the β-subunit. We show that gene transcription also requires the binding of Ca^{2+} to the channel pore and is calcium-influx independent. These results delineate Cav1.2–H-Ras interaction by extracellular signaling as a mode of rapid induction of gene transcription. They expand the repertoire of Cav1.2 metabotropic signaling triggered by depolarization-induced conformational changes, which require channel-pore occupancy and are calcium-influx independent.

Author contributions: E.S., M.T., and D.A. designed research; E.S., M.T., and D.M. performed research; E.S., M.T., and D.A. analyzed data; and M.T. and D.A. wrote the paper.

The authors declare no conflict of interest.

This article is a PNAS Direct Submission.

[1]To whom correspondence should be addressed. Email: daphne.atlas@mail.huji.ac.il.

This article contains supporting information online at www.pnas.org/lookup/suppl/doi:10.1073/pnas.1805380115/-/DCSupplemental.

Published online August 27, 2018.

We used Cav1.2-transfected HEK293 cells, which enabled us to monitor Cav1.2-mediated nuclear signaling activity in the absence of other VGCCs. Membrane targeting of the channel was determined by the high-resolution photoactivated-localization microscopy (PALM) using the Dronpa-tagged $\alpha_1$1.2 subunit, a reversibly switchable tetrameric photoactivatable fluorescent protein.

Cav1.2 and its Ca^{2+}-impermeable Cav1.2^{L745P} mutants provided insight into the Ca^{2+} dependency of the depolarization-triggered ERK/RSK/CREB pathway. Subsequent transcriptional activation of c-Fos and methyl-CpG-binding protein 2 (MeCP2) tested regulation of gene expression by a series of protein–protein interactions. A selective mutation within the alpha-interacting domain (AID) of $\alpha_1$1.2, which is known to interfere with intersubunit signaling of $\alpha_1$1.2 and β2b, was used to monitor signal transduction from $\alpha_1$1.2 via β2b and onto H-Ras. Cell-free binding of recombinant proteins and pulldown assays were used to show a physical interaction of the β2 subunit with H-Ras and Ras-GRF1 exchange protein in HEK293 cells or N-Ras in human neuronal SH-SY5Y cells. The data underline the ability of Cav1.2 to rapidly induce gene transcription in response to extracellular stimuli through propagating protein–protein interactions through β2b onto H-Ras. These interactions are independent of Ca^{2+} entry and provide insight into the role of the Ca^{2+}-bound channel pore in triggering ET coupling. Furthermore, these results extend our previous work implicating Ca^{2+} binding at the channel open pore during membrane depolarization as the signal for ES coupling (26) and EC coupling (21).

Results

Voltage-Gated Ca_V1.2 Channels Activate the ERK1/2–CREB Pathway. To assess the impact of Cav1.2 subunits on nuclear signaling, we monitored Ras/ERK/CREB activation in HEK293 cells transfected with cDNA consisting of the three channel subunits of Cav1.2: $\alpha_1$1.2, the pore-forming subunit; α2δ, the auxiliary peripheral membrane subunit; and β2b, the cytosolic subunit (Fig. 1). Cells were also transfected with different combinations of channel subunits: $\alpha_1$1.2/α2δ and $\alpha_1$1.2/β2b. Seventy-two hours after transfection, the cells were treated with either 2.5 mM KCl (basal) or depolarized by 70 mM KCl (70K) (dep) for 3 min.

Membrane depolarization triggered ERK1/2, RSK, and CREB phosphorylation in cells transfected with $\alpha_1$1.2/β2b/α2δ (Fig. 1). Net activation was calculated as the difference in activity induced by 70K (dep) and the basal activity (Fig. 1*B*, *Upper*). Strikingly, while cells expressing $\alpha_1$1.2/β2b (without α2δ), exhibited only a reduction in ERK1/2, RSK, and CREB phosphorylation, 60%, 50%, and 50%, respectively, compared with $\alpha_1$1.2/α2δ/β2b transfected cells, the ERK1/2 and CREB phosphorylation was virtually abolished in cells transfected with $\alpha_1$1.2/α2δ (without the β2b). These results indicate a crucial role of β2b in Cav1.2-driven gene activation (Fig. 1 *A* and *B*, *Lower*).

We then examined whether the absence of activity in cells expressing $\alpha_1$1.2/α2δ resulted from changes in Ca^{2+} influx. Elevation of intracellular calcium {$[Ca^{2+}]_i$} in response to membrane depolarization was recorded using the calcium fluorophore 4 (Fluo-4). No significant change in $[Ca^{2+}]_i$ rise was observed in cells expressing $\alpha_1$1.2/α2δ, $\alpha_1$1.2/β2b, or $\alpha_1$1.2/β2b/α2δ (*SI Appendix*, Fig. S1*A*). This is consistent with α2δ's ability to compensate for the β-subunit in $\alpha_1$1.2 trafficking to the membrane (27–29).

Channel targeting to the membrane was shown by the high-resolution PALM imaging technique (30) in the total internal reflection (TIRF) mode. It allowed visualization of the photoactivated Dronpa-tagged $\alpha_1$1.2 subunit at the plasma membrane of a single cell, in close proximity to the coverslip (up to ∼100 nm). Self-clustering distributions of Cav1.2 ($\alpha_1$1.2/α2δ/β2b), $\alpha_1$1.2/α2δ, or $\alpha_1$1.2/β2b were similar (*SI Appendix*, Fig. S1*B*). Channel expression was also monitored by confocal microscopy using Dronpa fluorescence of Dronpa-tagged $\alpha_1$1.2 (*SI Appendix*, Fig. S2*A*). We detected no significant fluorescence changes in cells transfected with Dronpa-tagged $\alpha_1$1.2 + α2δ or Dronpa-tagged $\alpha_1$1.2 + β2b.

Thus, the ERK/RSK/CREB signaling pathway, which is synchronized with channel openings (depolarization), requires extracellular Ca^{2+} (*SI Appendix*, Fig. S3), but is not correlated with elevated levels of intracellular Ca^{2+}.

MEK Inhibition Partially Blocks CREB Phosphorylation in Neuronal SH-SH5Y Cells. We showed inhibition of the ERK/CREB signaling by the dominant-negative mutant of H-Ras (Ras^{S17N}) and by selective inhibitors PLX4720 (0.5 μM), an inhibitor of the Ras-activated Raf serine/threonine kinase, and PD184,352 (2 μM), an inhibitor of MAPK/ERK kinase (MEK1/2) protein kinase (*SI Appendix*, Fig. S4*A*).

The complete blockade of the ERK/CREB pathway by PD184,352 in Cav1.2-transfected HEK293 cells indicates that nuclear signaling can be triggered largely through the Ras/MEK/ERK pathway. Neuronal cells harbor a variety of VGCCs, Ca_V1 channels that contribute to nuclear signaling at more negative potentials, −19 mV corresponding to 40 mM KCl (40K), or Ca_V2 channels at −9 mV corresponding to 60 mM KCl (60K). The effects of MEK inhibition on 40K- and 70K-triggered ERK1/2 and CREB phosphorylation were tested in human neuroblastoma SH-SY5Y cells (Fig. 2). Similar to HEK293 cells, ERK phosphorylation was completely blocked by PD184,352, while CREB phosphorylation was partially inhibited 45% in 40K and 65% in 70K (Fig. 2). Hence, CREB phosphorylation in neuronal cells expressing both Cav1 and Cav2 appears to be triggered both by a Ras/ERK-dependent and -independent signaling pathway (24). The complex nature of the neuronal cell, however, points out the difficulties in examining the Cav1.2-specific contribution to the molecular mechanism of nuclear signaling in these cells.

A Physical Interaction of the β2 Subunit with H-Ras and Ras/GRF1. The importance of β2b for ERK/RSK/CREB phosphorylation (Fig. 1) suggests a direct association of β2 with H-Ras and led us to explore whether β2b feeding into H-Ras could activate the ERK/CREB signaling pathway.

The possibility of a physical interaction between the β2 subunit and H-Ras was tested in cell-free binding. Purified His6-β2a (2 μg/mL) was immobilized onto Ni beads and mixed with the recombinant purified GST/Ras (1 μg/μL). GST/Ras was eluted from the His6-β2a-loaded Ni beads, but was significantly less in the eluant of the Ni beads without His6-β2a (Fig. 3*A*). Similarly, GSH-beads loaded with the recombinant protein GST/H-Ras (1 μg/μL) revealed bound recombinant His_6-β2a, whereas GSH-beads without GST/H-Ras displayed no binding (Fig. 3*B*). These demonstrate the ability of β2b to physically bind to the GDP form of H-Ras. A similar interaction of Cavβ with members of the H-Ras superfamily Rem, Rad, Rem2, and Gem/Kir (called RGK superfamily of Ras-related small GTPases), was previously reported (16, 31), and has been shown to affect long-term gene signaling (32).

Ras is activated by a Ras-specific guanine nucleotide exchange factor (Ras/GRF1), a protein that exchanges GDP with GTP (33). For testing whether the H-Ras activation is mediated through β2a interaction with the Ras/GRF1, human neuronal SH-SY5Y cell lysates were incubated with recombinant His6-tagged β2a (see above). Ras/GRF1 identified by CDC25 antibodies (34) was pulled down by His6-tagged β2b upon adding Ni beads, while no Ras/GRF1 was found in cell lysates exposed to Ni beads free of His6-β2a (Fig. 3*C*). H-Ras pulled down β2a (Fig. 3*D*), and β2a pulled down N-Ras, the dominant Ras isoform in these cells (Fig. 3*E*).

Altogether, the pulldown experiments in neuronal cells show the capability of β2b to interact directly with H-Ras and also with Ras/GRF1. The physical interaction of β2a with H-Ras, and/or Ras/GRF1 suggests that Cav1.2-driven ET coupling is likely governed by a series of protein–protein interactions, initiated during membrane depolarization in $\alpha_1$1.2. These findings open

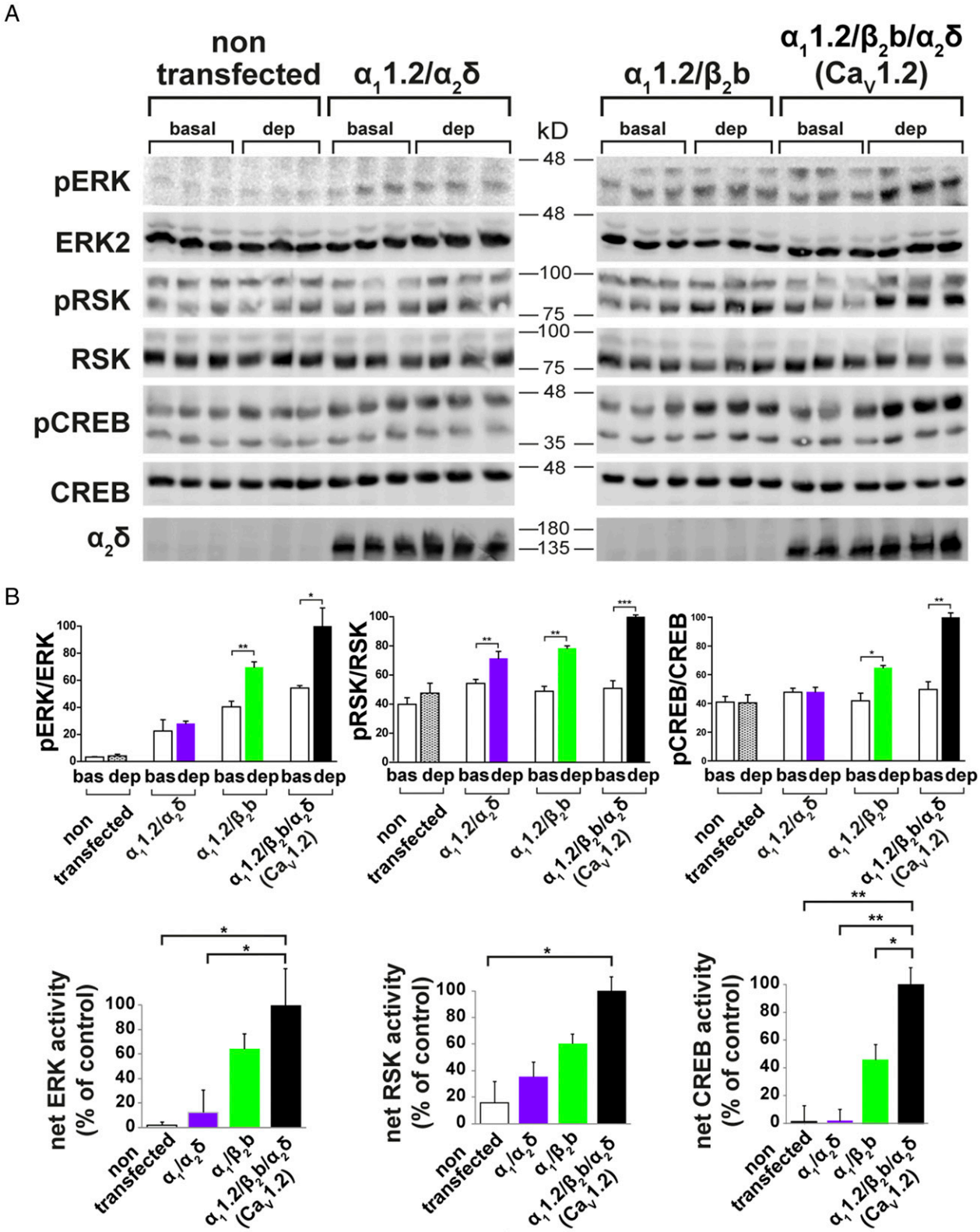

Fig. 1. The β-subunit is required for ERK/CREB activation in Cav1.2 expressed in HEK293 cells. (*A*) HEK293 cells transiently transfected with Cav1.2 channel subunits $\alpha_1$1.2/α2δ/β2b (black), $\alpha_1$1.2/α2δ (violet), or $\alpha_1$1.2/β2b (green), as indicated. After 72 h, the cells were treated with 2.5K (nondepolarizing) or 70K (depolarizing; dep) solutions for 3 min. The cells were harvested, and proteins in cell extracts were resolved by SDS/PAGE and analyzed by Western blot analysis (*Materials and Methods*). Transfection efficiency was monitored using anti-α2δ antibodies. (*B*) Quantification of ERK1/2, RSK, and CREB phosphorylation was performed by Western blot analysis, densitometry, and plotted with a linear regression program. Net phosphorylation was calculated by subtracting basal phosphorylation observed in cells treated with a nondepolarizing solution (basal) from phosphorylation triggered by depolarizing solution (dep) in triplicates. The values shown are averages (±SEM) of three independent experiments normalized with the corresponding nonphosphorylated protein. Student's *t* test (two populations) was performed. $*P < 0.05$, $**P < 0.01$, $***P < 0.005$.

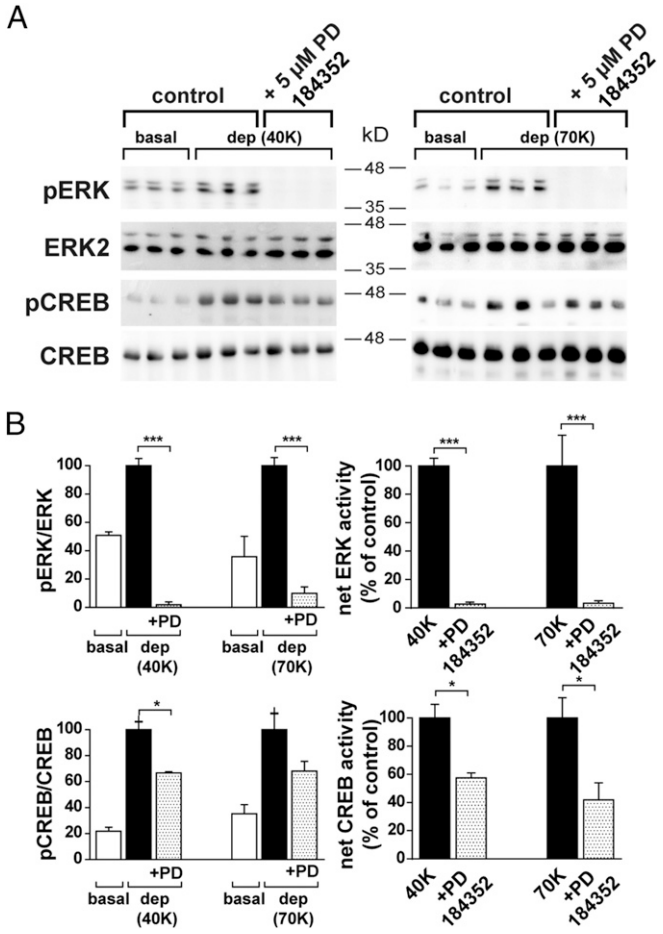

Fig. 2. CREB phosphorylation in SH-SY5Y cells is triggered by membrane depolarization via ERK-dependent and -independent pathways. (*A*) SH-SY5Y cells treated with or without the 5 μM PD184,352 inhibitor were depolarized by 40 mM (40K; dep) or 70 mM KCl (70K; dep) and phosphorylation of ERK and CREB was monitored by Western blot analysis. (*B*) Quantification of the basal phosphorylation of ERK1/2 and CREB, 40K, and 70K (*Left*). One-way ANOVA was used to determine statistically significant differences. $*P < 0.05$, $**P < 0.01$, $***P < 0.001$. Net phosphorylation was calculated by subtracting basal phosphorylation (*Right*). The values shown are averages (±SEM) of triplicates carried out in three independent experiments using different cell batches, normalized with the corresponding nonphosphorylated protein; Student's *t* test (two populations) was performed. $*P < 0.05$, $***P < 0.005$.

more questions as to the GTP/GDP dependency of the interaction, whether GTP binding disrupts H-Ras–β2 associations, and how the Cav1.2–β2 interaction results in Ras activation.

Nuclear Signaling via Cav1.2 Requires Crosstalk Between $\alpha_1$1.2 and β2b. The physical and functional interaction of β2b with H-Ras and Ras/GRF1 led us to propose a model in which the coordinated phosphorylation of the ERK1/2–CREB pathway originates at $\alpha_1$1.2 and is conveyed to H-Ras through β2b. The β-subunit has been shown to modulate calcium channel kinetic parameters through a high-affinity interacting binding domain at the α_1 subunit (AID), located in the I–II linker of $\alpha_1$1.2 (35–37). A single point mutation W440A within the AID consensus sequence (Fig. 4*A*) strongly mitigates $\alpha_1$1.2 interaction with β, increasing current amplitude (28, 29). We used the $\alpha_1 1.2^{W440A}$ mutant that disrupts the interaction between $\alpha_1$1.2 and β2b, testing the impact of crosstalk between these two channel subunits on nuclear activation (Fig. 4). Channel expression was monitored by confocal microscopy using the photoactivated Dronpa fluorescence of Dronpa-tagged $\alpha_1$1.2. No significant changes in fluorescence were detected in cells transfected with either Dronpa-tagged $\alpha_1$1.2 or Dronpa-tagged $\alpha_1 1.2^{W440A}$ (*SI Appendix*, Fig. S2*B*, *Left*). To determine membrane targeting of the mutated channel ($\alpha_1 1.2^{W440A}$/β2b/α2δ; Xam1.2^{w440A}) we applied the TIRF mode of the high-resolution PALM imaging technique, using the Dronpa-tagged $\alpha_1 1.2^{W440A}$ (30). Self-clusters of Cav1.2^{W440A} were distributed on the cell membrane Fig. 4*B*, similar to WT Cav1.2 cluster distribution.

We then compared depolarization-triggered ERK/RSK/CREB activation in cells expressing Cav1.2^{W440A} and Cav1.2^{W440A}. The W440A mutant nearly abolished (>90%) the 70K (dep)-induced ERK1/2, RSK, and CREB activation compared with the WT channel (Fig. 4*C*).

The loss of ERK/CREB phosphorylation by disrupting a functional interaction between $\alpha_1$1.2 and β2b confirms the lack of

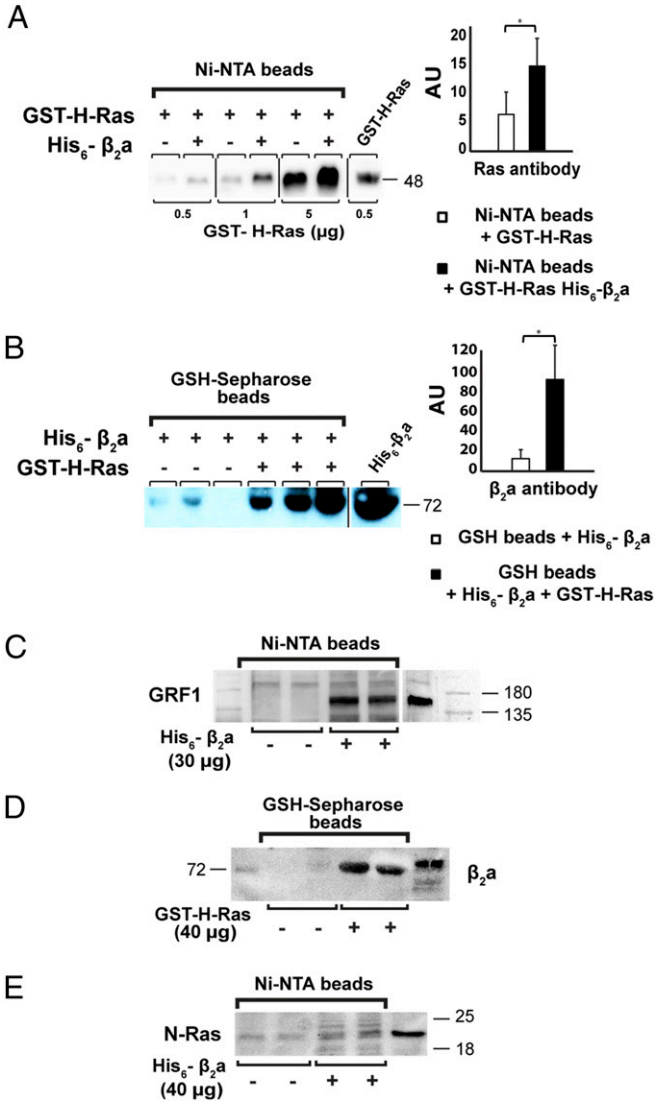

Fig. 3. The Cavβ2a binds H-Ras in in vitro studies. (*A*) Cell-free binding of GST/Ras fusion protein with His$_6$β2a protein immobilized on Ni-NTA beads or (*B*) His$_6$β2a protein binding to H-Ras immobilized on GSH–Sepharose beads performed as indicated (*Materials and Methods*). (*C*) Pulldown of Ras/GRF1 with His$_6$β2a in neuronal human SH-SY5Y cells. (*D*) Pulldown of β2a by GST/H-Ras in SH-SY5Y cells and (*E*) pulldown of N-Ras by His$_6$β2a in SH-SY5Y cells. Each experiment was repeated three times using different batches of SH-SY5Y cells. $*P < 0.01$.

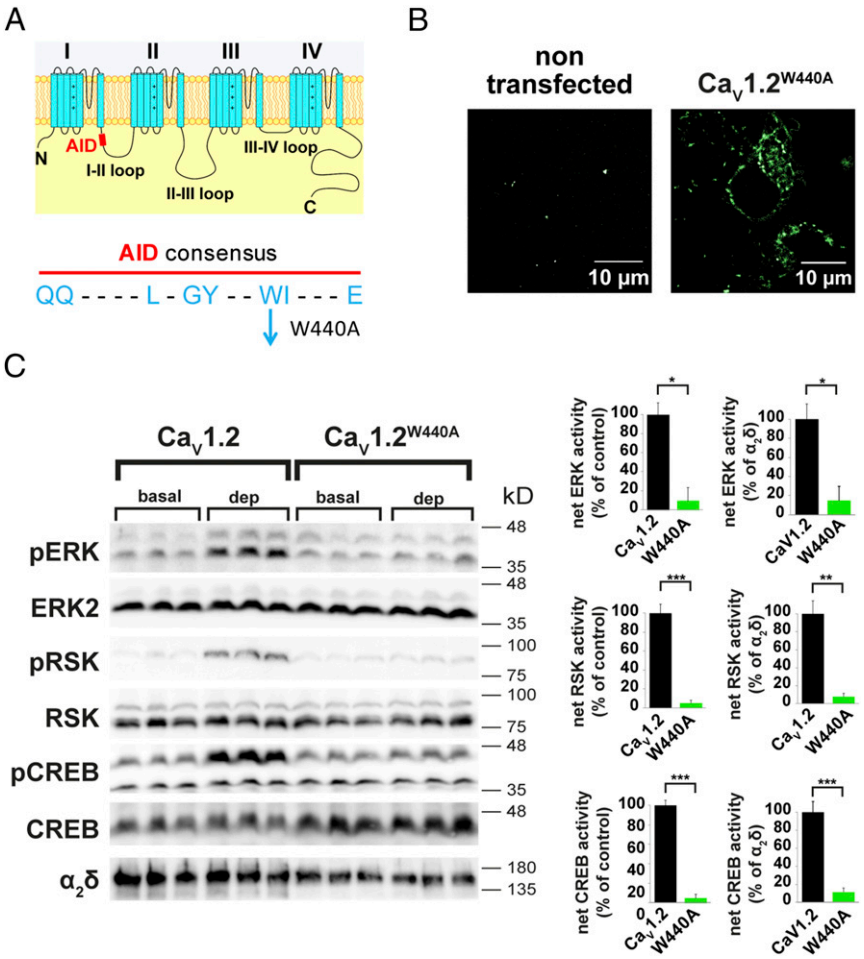

Fig. 4. Disruption of $\alpha_1$1.2–β2b interaction by the W440A mutation at the AID motif obliterates Cav1.2-driven ERK, RSK, and CREB activation. (*A*, *Left*) Schematic view of $\alpha_1$1 subunit of Ca_V1 and the location of the AID within the I–II linker (marked in red). (*A*, *Right*) The W440A mutation at the highly conserved AID consensus sequence of voltage-activated Ca_V1 α_1 subunits. (*B*) PALM images of nontransfected HEK293 cells, and Cav1.2 ^{W440A} (Dronpa-tagged $\alpha_1$1.2^{W440A}/β2b/$\alpha_2\delta$)-expressing HEK293 cell. (Scale bar, 10 µm.) (*C*, *Left*) HEK293 cells transfected with WT Cav1.2 ($\alpha_1$1.2/β2b/$\alpha_2\delta$) or the mutated channel Cav1.2^{W440A}. Seventy-two hours later, the cells were stimulated with a nondepolarizing or depolarizing solutions for 3 min. Activation of ERK, RSK, and CREB was detected using the corresponding phosphoproteins (see legend Fig. 1*A*). (*C*, *Right*) Phosphorylation was quantified by densitometry and plotted with a linear regression program. The plotted values are averages (±SEM) of three independent experiments normalized to the corresponding nonphosphorylated proteins, or $\alpha_2\delta$ subunit antibodies. All experiments were done in triplicate transfections and performed three times using different cell batches. Net phosphorylations are averages (±SEM) of triplicates carried out in three independent experiments, normalized with the corresponding nonphosphorylated protein. Student's *t* test (two populations) was performed for 70K-treated cells. $^*P < 0.05$, $^{**}P < 0.01$, $^{***}P < 0.001$.

activation observed in the absence of β2b (Fig. 1). It strongly supports the idea that depolarization-induced conformational changes at $\alpha_1$1.2 drives ET coupling via the β2b subunit. Since the W440A mutation does not interfere with Ca^{2+} influx (28, 29), these results further indicate that Ca^{2+} entry during depolarization is not sufficient for triggering nuclear activation. A precedent for such a mechanism using the β-subunit was demonstrated when a signal was conveyed from the voltage-sensing regions of the skeletal $\alpha_1$1.1 to the pore region of the ryanodine receptor by means of β1b (38). Also, members of the Ras superfamily, such as RGKs (Rem, Rad, Rem2, and Gem/Kir), which exhibit conserved structural features that distinguish them from the other Ras proteins, have been shown to modulate Cav1 activity through binding to the β-subunit (16, 32, 39).

The Role of CaM in ERK/CREB Activation. To further investigate the Ca^{2+} dependency of Ca_V1.2-mediated Ras/ERK/CREB pathway, we examined CaM inhibitors and Ca^{2+}/CaM binding to the IQ motif at the C terminal of $\alpha_1$1.2 (*SI Appendix*, Fig. S5*A*).

We showed that trifluoperazine, a Ca^{2+}/CaM inhibitor, or selective CaN inhibitors cyclosporin A (CsA) and FK506, displayed no significant reduction in Cav1.2-driven ERK, RSK, or CREB phosphorylation. The channel mutant $\alpha_1$1.2^{I1624A}/β2b/α2δ that prevents Ca^{2+}/CaM binding to the mutated IQ motif exhibited a small reduction in ERK1/2 phosphorylation compared with WT Cav1.2-expressing cells, and no effect on RSK, or CREB phosphorylation (*SI Appendix*, Fig. S5*C*). These results negate a significant impact of Ca^{2+}-activated pathways such as Ca^{2+}/CaM-dependent kinase on ET coupling in Cav1.2-transfected HEK293 cells.

ET Coupling Is Triggered by a Sequential Series of Protein–Protein Interactions Initiated by Ca^{2+} Binding at the Open Channel Pore. Cav1 channels are responsible for the majority of depolarization-induced gene expression, yet they account for a small fraction of bulk calcium flux in neurons (25). For clarifying the need of Ca^{2+} entry through Cav1.2 in triggering nuclear signaling, we used a Ca^{2+}-impermeable Cav1.2 mutant. Separating the Ca^{2+}-binding function at the open pore from Ca^{2+} entry allowed us to assess

the impact of Ca^{2+} binding at the selectivity filter from the ensuing Ca^{2+} influx. The Ca^{2+}-impermeable channel was generated by a single point mutation introduced at the pore forming subunit (L745P; $\alpha_1 1.2^{L745P}$), corresponding to the rabbit L775P mutation (20, 21, 40). Patch clamp studies in single tsA-201 cells have shown targeting of the L775P impermeable channel mutant to the cell membrane (40). The rabbit $Cav1.2^{L775P}$ mutant supports depolarization-induced secretion of catecholamines in adrenal medullary cells and contraction in neonate cardiomyocytes (20, 21).

We used PALM imaging in the TIRF mode, monitoring the photoactivated Dronpa-tagged $\alpha_1 1.2^{L745P}$ to confirm membrane targeting of $\alpha_1 1.2^{L745P}/\beta 2b/\alpha 2\delta$ in HEK293 cells. As shown in Fig. 5*A*, distribution of Dronpa-tagged $\alpha_1 1.2^{L745P}$ self-clusters at the plasma membrane was similar to Dronpa-tagged $\alpha_1 1.2$ (30). Also the expression of the L745P mutant and WT Cav1.2 was similar, as imaged by confocal microscopy of the Dronpa-tagged $\alpha_1 1.2^{L745P}$ mutant (*SI Appendix*, Fig. S2*B*, *Right*).

To confirm, calcium impermeability of the $Cav1.2^{L745P}$ mutant was determined by a calcium colorimetric assay, and confocal imaging (Fig. 5 *B* and *C*). An increase in Fluo-4 fluorescence, measured every 30 s for 5 min, was observed in WT Cav1.2-transfected cells but not in $Cav1.2^{L745P}$-transfected cells or in the nontransfected cells (Fig. 5*B*). Similarly, confocal-imaging showed an increase in Fluo-4 fluorescence in WT Cav1.2-transfected cells, during depolarizing (dep), and no increase in Fluo-4 fluorescence was detected upon depolarization of $Cav1.2^{L745P}$-transfected HEK293 cells, confirming Ca^{2+} impermeability of the channel mutant (Fig. 5*C*).

Next we showed that without conducting Ca^{2+}, the impermeable channel $Cav1.2^{L745P}$, responded to membrane depolarization and mediated a significant increase in phosphorylation of ERK1/2, RSK, and CREB (Fig. 5 *D* and *E*). The extent of phosphorylation, however, was 40–60% smaller compared with the WT channel (Fig. 5*E*). This result could indicate that maximal activation requires a Ca^{2+}-dependent component (*Discussion*).

Similar to the WT channel, depolarization-induced phosphorylation via $Cav1.2^{L745P}$ was virtually abolished by verapamil (20 μM), a selective Cav1.2 blocker that binds at the aperture of the open pore, or by Cd^{2+} (200 μM), a general VGCC pore blocker that prevents $Ca_V1.2$ from Ca^{2+} conducting without affecting depolarization or voltage-dependent gating (41, 42) (Fig. 5 *D* and *E*). Furthermore, FPL-64176 (1 μM), a Cav1 channel agonist, known to increase the open probability of Cav1 channels, potentiated both the WT and the impermeable channel-triggered phosphorylation of ERK1/2, RSK, and CREB (Fig. 5 *D* and *E*).

These findings indicate that excitation-response coupling of the ERK/CREB pathway engages a Ca^{2+}-bound channel pore in a conducting mode, but is Ca^{2+}-influx independent. Future experiments should clarify whether a rapid signaling in neurons induced by conformational changes at Cav1.2 before Ca^{2+} influx might be involved in switching on transcription already primed for activation (43) and provide a selective signaling mode over Ca^{2+}-activating pathways.

Mutating the glutamate residues (EEEE motif) comprising the Cav1.2 selectivity filter, disrupts Ca^{2+} binding and impairs ion selectivity (42, 44, 45). If the open selectivity filter must be occupied by two calcium ions to achieve a conducting mode to allow gene activation, we hypothesized that mutating the EEEE motif would compromise the activity. A single point mutation E363A (E/A), and a double point mutation E363A/E1115A (EE/AA) were introduced at the EEEE motif of the Ca^{2+}-impermeable pore-forming subunit ($Cav1.2^{L745P}$; Fig. 6). Depolarization of cells expressing these mutants showed reduced levels of ERK/RSK/CREB activation (>80%) by the single pore mutant $\alpha_1 1.2^{L745P/E363A}/\beta 2b/\alpha 2\delta$ (EA), and virtually no activation by the double pore mutant $\alpha_1 1.2^{L745P/E363A/E1115A}/\beta 2b/\alpha 2\delta$ (EE/AA) (Fig. 6*A*). The loss of ET coupling by specifically restricting Ca^{2+} binding at the channel pore strongly supports our model in which Ca^{2+} residing at the open EEEE motif is essential for nuclear activation.

The impermeable and the two pore mutants also tested the role of the Ca^{2+}-bound channel in mediating transcription activation, by following the expression of CREB-regulated c-Fos and MeCP2.

The expression of c-Fos (Fig. 6*B*) and MeCP2 (Fig. 6*C*) was monitored 60 min after a 3-min stimulation period (dep). Both WT and $Cav1.2^{L745P}$ elevated the expression of c-Fos and MeCP2. The single E363A mutant of the impermeable channel, $\alpha_1 1.2^{L745P/E363A}$ partially reduced, while the double mutant $\alpha_1 1.2^{L745P/E363A/E1115A}$ virtually obliterated gene expression. These data confirm the correlation between triggering gene expression and Ca^{2+} binding at the channel pore as opposed to Ca^{2+} influx.

Discussion

In the present study, we have demonstrated that the VGCC $Ca_V1.2$ couples membrane depolarization to transcriptional activation via the ERK/CREB pathway independently of Ca^{2+} entry. Activation requires Ca^{2+} binding at the pore and a direct interaction of H-Ras with the Cavβ2 subunit. These findings suggest that a highly concerted signal that originates during membrane depolarization at $\alpha_1 1.2$ is conveyed to H-Ras via a direct interaction with β2b. The binding of β2b to H-Ras facilitates gene activation via the Ras/ERK/CREB signaling pathway.

This conformational-triggered series of protein–protein interactions underscores a mode of gene regulation by extracellular signals and could have broad implications for understanding the rapid induction of nuclear transcription factors primed for gene activation (43, 46, 47).

Cav1 Channel Signaling to the Nucleus Is Driven by a Direct Interaction of Cav1.2 β2 Subunit with H-Ras. Because membrane depolarization causes Cav1.2 to introduce calcium into the cells, prior studies have focused on the idea that genes are activated by elevated $[Ca^{2+}]_i$. However, it was also shown that gene activation efficacy is not directly correlated with Ca^{2+} influx (8, 25).

Given these apparent conflicting characteristics of the process and the importance of VGCC-activating nuclear signaling, we explored Cav1.2-driven ERK/CREB activation by brief depolarization of Cav1.2-transfected HEK293 cells.

The expression of $\alpha_1 1.2/\beta 2b/\alpha 2\delta$, the three channel subunits of Cav1.2, exhibits a significant activation of the ERK/RSK/CREB pathway. In contrast, activity is virtually abolished by excluding the β2b subunit. The omission of β2b shows no change in either global $[Ca^{2+}]_i$ using Fluo-4 imaging, nor does it affect channel distribution on the cell surface, shown by high resolution of PALM imaging of Dronpa-tagged $\alpha_1 1.2$. These results highlight a critical role of β2b in Cav1.2-mediated nuclear activation, emphasizing a conformational signaling role for Cav1.2, which is independent of Ca^{2+} influx.

The cell-free binding of recombinant proteins revealed the ability of β2b to bind to H-Ras. In complementary pulldown experiments of human neuronal SH-SY5Y cells, β2b pulled down N-Ras, as well as Ras/GRF1, the Ras GDP/GTP exchanger. This direct physical interaction of β2b with H-Ras underscores the importance of β2b–H-Ras interaction in transcriptional regulation in neuronal cells. A functional association of β2b with RGKs, members of the super-Ras family, has been previously described (39, 48–53).

The decrease in ERK/RSK phosphorylation caused by Ras^{S17N}, the dominant-negative H-Ras mutant, further confirmed the central role of H-Ras in mediating Cav1.2-triggered nuclear signaling (8, 14). Consistent with the inhibitory effect of Ras^{S17N}, the obliteration of depolarization-induced ERK/RSK/CREB phosphorylation by the selective Raf (MAPKKK), and MEK1/2 (MAPKK) inhibitors, PLX4720 and PD184352, respectively, highlights the

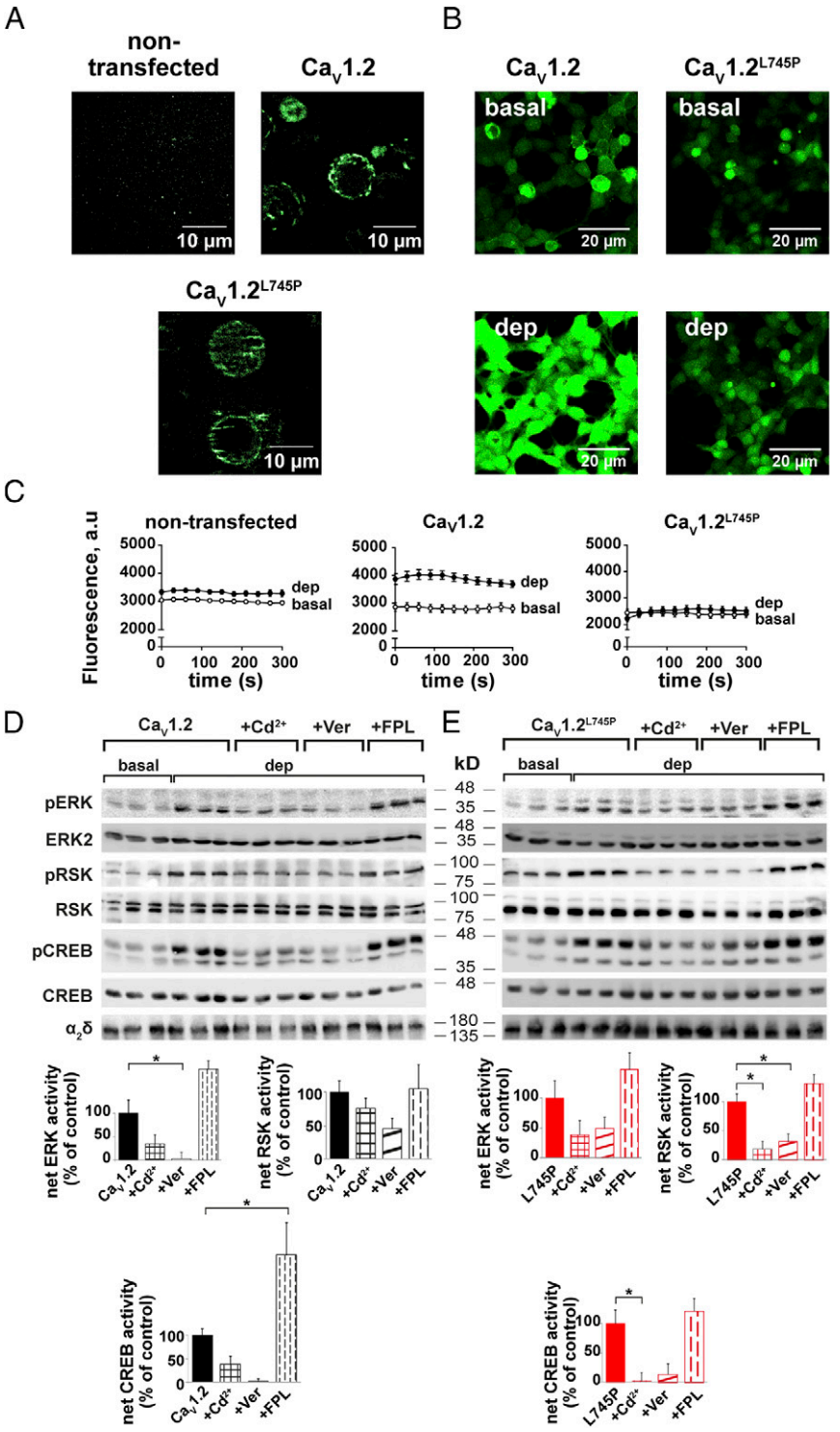

Fig. 5. The Ca^{2+}-impermeable channel Cav1.2^{L745P} activates the ERK/RSK/CREB signaling pathway. (*A*) PALM images of HEK293 cells transiently transfected with WT Cav1.2 and Ca^{2+}-impermeable channel Cav1.2^{L745P}. A representative of a nontransfected HEK293 cell, a cell expressing WT Cav1.2 (Dronpa-tagged $\alpha_1$1.2/β2b/α_2δ), or Cav1.2^{L745P} (Dronpa-tagged $\alpha_1$1.2^{L745P}/β2b/α2δ) were taken 72 h after transfection. (Scale bar, 10 µm.) (*B*) Confocal imaging of Ca^{2+} elevation in HEK293 cells performed using the D-Eclipse C1 imaging system. HEK293 cells transiently transfected with WT Cav1.2 or Cav1.2^{L745P} were pulsed 72 h later with nondepolarizing (basal) or depolarizing (dep) solutions for 3 min. Fluo-4 fluorescence in control and in stimulated cells is shown in exemplary cells. The assay was performed in triplicate in three independent experiments. (*C*) Intracellular Ca^{2+} {$[Ca^{2+}]_i$} rise was measured by Fluo-4 AM kinetics (excitation: 490 nm; absorbance: 525 nm). HEK293 cells transiently transfected with WT Cav1.2 or Cav1.2^{L745P} were stimulated as above. The reaction rate of Fluo-4 AM kinetics was measured at 10 time points (every 30 s for 300 s). The values of net $[Ca^{2+}]_i$ are averages (±SEM) of three independent experiments. ERK1/2, RSK, and CREB phosphorylation was triggered as above in cells expressing WT Cav1.2 (*D*) and Ca^{2+}-impermeable Cav1.2^{L745P} (*E*), without or with Cd^{2+} (200 µM), verapamil (Ver; 10 µM), or FPL-64176 (1 µM). Phosphorylation was quantified by densitometry and plotted with a linear regression program. Net phosphorylation was calculated (Fig. 1). The plotted values are averages (±SEM) of three independent experiments normalized to nonphosphorylated proteins using the corresponding antibodies. Experiments were done in triplicate transfections and performed three times using different cell batches. One-way ANOVA was used to determine statistically significant differences. *$P < 0.05$.

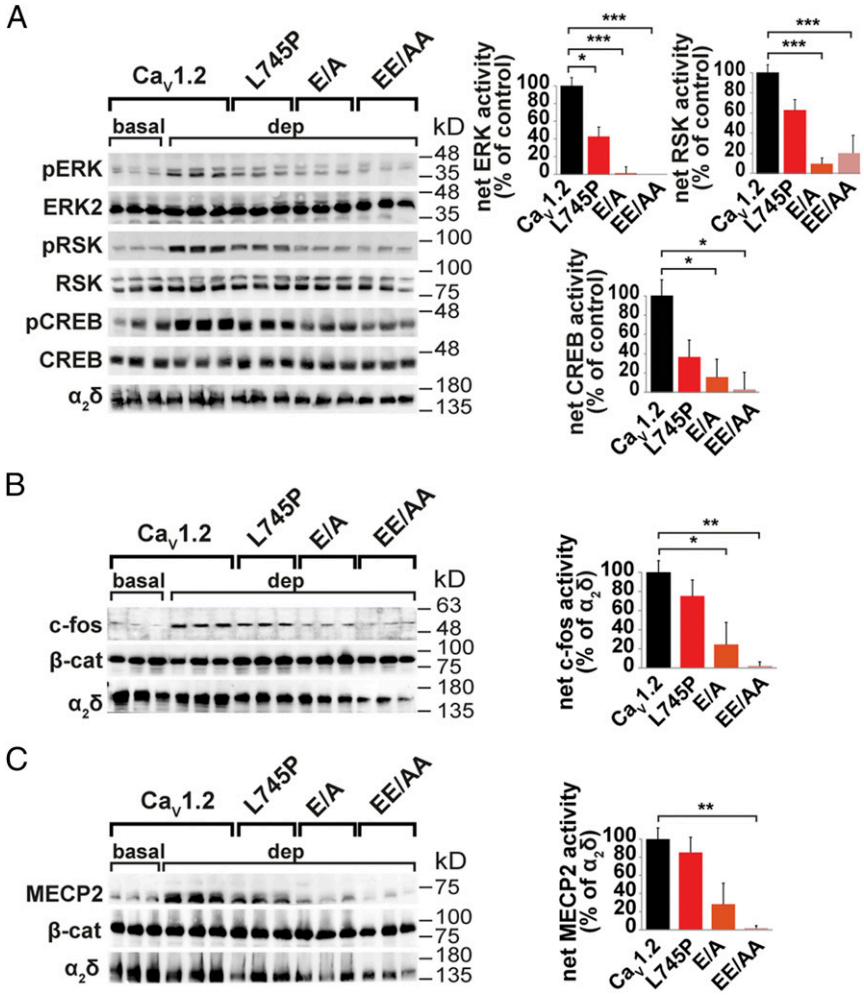

Fig. 6. Mutating Ca^{2+}-binding site of Ca^{2+}-impermeable Cav1.2^{L745P} pore prevents nuclear activation. (*A*) WT Cav1.2 ($\alpha_1$1.2/β2b/α2δ) or Cav1.2^{L745P} ($\alpha_1$1.2^{L745P}/β2b/α2δ) and the two pore mutants $\alpha_1$1.2$^{L745P/E363A}$/β2b/α2δ, and $\alpha_1$1.2$^{L745P/E363A/E1115A}$/β2b/α2δ were pulsed with nondepolarizing (basal) or depolarizing (70K; dep) solutions for 3 min. Phosphorylation of ERK1/2, RSK, and CREB was monitored by Western blot analysis and quantified (*Lower*). The plotted values are averages (±SEM) of three independent experiments normalized to nonphosphorylated proteins using the corresponding antibodies. Student's *t* test (two populations) was performed for 70K-stimulated cells. $*P < 0.05$, $**P < 0.01$, $***P < 0.005$. (*B*) The WT Cav1.2 and Cav1.2^{L745P} and the pore-mutants channels $\alpha_1$1.2$^{L745P/E363A}$/β2b/α2δ- and $\alpha_1$1.2$^{L745P/E363A/E1115A}$/β2b/α2δ-expressing cells were pulsed as indicated above (*A*). Expression of c-Fos (*B*) and MeCP2 (*C*) was monitored by Western blot analysis and quantified according to α2δ expression. All experiments were done in triplicate transfections and performed three times using different cell batches. One-way ANOVA was performed to determine statistically significant differences for K70-stimulated cells. $*P < 0.05$, $**P < 0.01$, $***P < 0.001$.

major role of H-Ras in Cav1.2-induced ET coupling. Although the pulldown of Ras/GRF1 by β2b in neuronal cells leaves open the question concerning the nature the GDP/GTP exchange activity required for H-Ras activation by β2b (7, 33), the dominant negative effects of Ras^{S17N} on nuclear signaling give further credence to β2 functional association with the Ras GRF1/Ras exchange system, schematically shown in Fig. 7. A detailed characterization of H-Ras activation via β2b and its impact in various neuronal cell systems will require further studies.

In SH-SY5Y cells, which express in addition to Cav1, neuronal Cav2 channels, CREB activation persists, even if the MEK/ERK pathway is completely repressed by a selective inhibitor. These results are consistent with previous studies, demonstrating that CREB phosphorylation in neuronal cells could be triggered via other channels and through other biochemical pathways such as the calcium-CaMKII system (24).

To further explore the role of β2b in translating stimulus features of $\alpha_1$1.2 into activity-dependent gene induction, we disrupted the interaction between these two channel subunits. Functional and structural studies have shown that $\alpha_1$1.2 binds β2b at the highly conserved AID domain (35–37, 54). We introduced a single point mutation W440A within the AID helix. This mutation is known for disrupting the crosstalk of $\alpha_1$1.2 with β2b without affecting Ca^{2+} influx (28). Upon membrane depolarization, cells expressing Cav1.2^{W440A} mutant failed to activate the ERK/RSK/CREB pathway. These results highlight β2b as a molecular linker in Cav1.2-mediated nuclear signaling. There is precedent for this concept. Targeting of β_4 subunit to neuronal nuclei has been suggested to be responsible for coupling neuronal excitability to gene expression (55). Also β1b direct interaction with RyR1 has been found essential for the Ca$_V$1.1–RyR1 coupling mechanism (56, 57). Taken together, our results delineate a mechanism of gene activation, in which a signal is transmitted from the $\alpha_1$1.2 to the β2b subunit, reminiscent of EC coupling in skeletal muscle.

Depolarization-Driven Activation of the ERK/RSK/CREB Pathway Is Dependent on Ca^{2+} Occupancy of the Open Channel Pore. The Cav1-type channel, in contrast to the neuronal type Cav2, dominates the majority of depolarization-induced gene expression in neurons, even though it accounts for a small fraction of total

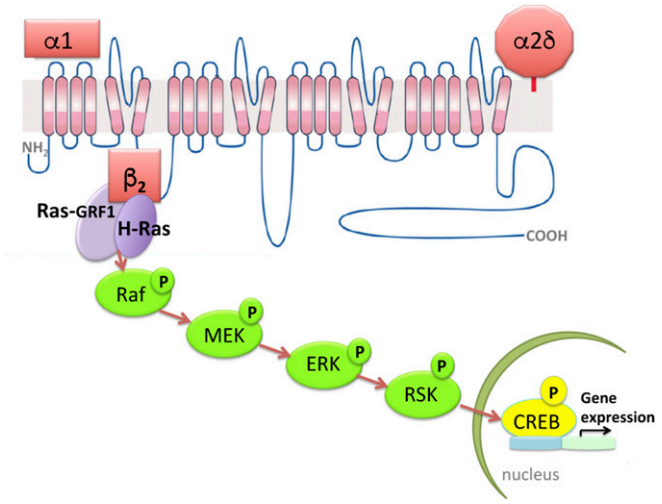

Fig. 7. Proposed model for depolarization-triggered activation of the ERK/CREB pathway via a direct interaction of the intracellular β2b with H-Ras. Upon neuronal stimulation by membrane depolarization, the $\alpha_1$1.2 pore-forming subunit of the L-type channel Cav1.2 conveys a concerted signal from the multi-Ca^{2+} ion-bound pore to the β_2 subunit. The β_2 subunit interacts directly with H-Ras and H-Ras/GRF1. Activated H-Ras initiates the phosphorylation of Raf, and through the MEK/ERK/RSK/CREB pathway, triggers signaling to the nucleus. $\alpha_1$1.2, pore-forming subunit; α2δ, extracellular subunit; β_2, intracellular subunit.

calcium entry. This apparent lack of correspondence between Ca^{2+} influx and transcriptional activation (25) has been previously explained by the intrinsic gating advantage of Cav1 and the Ca^{2+} nanodomain interaction with locally recruited CaMKII (24).

Therefore, we sought to analyze these long-standing contradictory characteristics of Ca^{2+}-dependent gene activation.

To distinguish between ET coupling induced by Ca^{2+} binding at the channel pore or by Ca^{2+} influx, we used a Ca^{2+}-impermeable channel mutant, $\alpha_1 1.2^{L745P}$ (40). Upon membrane depolarization, this channel, which retains voltage sensitivity and Ca^{2+} binding at the open selectivity filter (20), induced ERK, RSK, and CREB phosphorylation. The mutant channel also elevated the expression of CREB-regulated transcription factors c-Fos and MeCP2. These results provide strong evidence for the impact of Ca^{2+} occupancy of the open pore in triggering ET coupling. We observed no effect of trifluoperazine, a Ca^{2+}/CaM inhibitor, or calcineurin inhibitor on Cav1.2-triggered ERK/CREB activation, and no change in activation from WT channel was observed by expressing the IQ motif mutant $Cav1.2^{I1624A}$ that does not bind calmodulin (*SI Appendix*, Fig. S5). Hence, more studies are required to understand the contribution of the β-subunit, CaMK, and CaMKII activation to ET coupling.

Support for Ca^{2+} influx-independent ET coupling has been demonstrated also in vivo (32). In these studies, the dendritic retraction relies on long-term effects of Ca^{2+} flux-independent gene activation in the Timothy channel. Activation is triggered by conformational changes induced during membrane depolarization, activating the RhoA signaling via the small G protein Gem (32). These studies give additional credence to our proposed conformational coupling model that triggers gene activation via a cascade of protein–protein interactions.

Our proposed Ca^{2+}-influx independency of β2b-mediated ET coupling is reminiscent of EC coupling in the skeletal muscle in which the convergence of conformational coupling between the $Ca_V1.1$ and RyR1 via β1a, is also Ca^{2+}-influx independent (38, 57–61). Ca^{2+} binding or transition through the pore of $\alpha_1$1.1 was suggested to alter the skeletal $Ca_V1.1$ conformation to modulate intracellular signal transduction events (62).

The impact of Ca^{2+} binding at the channel pore on nuclear activation was further assessed using the Ca^{2+}-pore mutants of the Ca^{2+}-impermeable mutant $\alpha_1 1.2^{L745P/E363A}$ or $\alpha_1 1.2^{L745P/E363A/E1115A}$. These mutants at the EEEE motif, which constitutes the Ca^{2+} Cav1.2-binding site at the pore and determines Ca^{2+} selectivity (45), resulted in a significant decrease in ERK/RSK/CREB activities. Crippling of the Ca^{2+}-binding site of the Ca^{2+}-impermeable channel by these mutants is also correlated with failure to activate CREB-regulated c-Fos and MeCP2, lending further support for the importance of multiple Ca^{2+} occupancy of the open pore as the primary signaling event.

Structural studies have shown that the KcsA K^+ channel selectivity filter undergoes conformational change upon transition from a closed to an open state, during which the selectivity filter atoms are in direct contact with bound ions (63, 64). By analogy, a conformational change during Ca^{2+} binding at the EEEE motif could, via β2b and subsequently H-Ras, trigger signaling to the nucleus. This transition from a nonconductive to the conductive conformation during Ca^{2+} occupancy of the open channel has previously been shown to trigger excitation secretion and excitation contraction via conformational coupling through the II–III linker of the $\alpha_1$1.2 subunit (21–23, 26, 58, 59, 65).

In summary, these results provide evidence for the idea that membrane depolarization couples Ca1.2 to gene activation by engaging Ca^{2+}-bound open pore to initiate a direct β2b interaction with H-Ras. This series of protein–protein interactions represents a mode of a Cav1.2 selective mechanism of gene activation with a potential to give insight into rapid signaling in neuronal cells. The explicit implication of our results highlights Cav1.2 in its role as a calcium binding protein and expands the repertoire of signaling induced by Cav1.2-conformational changes prior to and independent of Ca^{2+} influx.

Materials and Methods

For a complete description of materials, transfection, expression of proteins, protein purification, Western blot analysis, and colorimetric and fluorescent measurements please refer to *SI Appendix*.

Cells. HEK293 cells were cultured in DMEM plus 10% FCS, 100 units/mL penicillin, 3 mM glutamine–alanine, and 1 μg/mL streptomycin at 37 °C in a humidified atmosphere with 5% CO_2.

Human neuroblastoma SH-SY5Y cells were cultured in DMEM:F12 (1:1) containing 10% FBS, 100 units/mL penicillin, 3 mM glutamine–alanine, and 1 μg/mL streptomycin at 37 °C with 5% CO_2.

Constructs. The α-subunits of WT and $\alpha_1$1.2 and $\alpha_1$1.2 mutants, $\alpha_1 1.2^{L745P}$ $\alpha_1 1.2^{W440A}$, $\alpha_1 1.2^{I1624A}$, $\alpha_1 1.2^{L745P/E363A}$, and $\alpha_1 1.2^{L745P/E363A/E1115A}$, were tagged with Dronpa, a reversibly switchable photoactivatable fluorescent protein; $GFP\text{-}Ras^{S17N}$.

Membrane Depolarization and ERK–RSK and CREB Activation. Before depolarization, the cells were starved for 2 h in DMEM supplemented with 2 mM L-alanyl glutamine. Subsequently, an equal volume was added of either low potassium 2.5 mM (basal) (125 mM NaCl, 30 mM glucose, 1 mM $MgCl_2$, 2 mM $CaCl_2$, 40 mM $NaHCO_3$, 1 mM NaH_2PO_4) or depolarized by high potassium K70 (dep) (135 mM KCl, 30 mM glucose, 1 mM $MgCl_2$, 2 mM $CaCl_2$, 40 mM $NaHCO_3$, 1 mM NaH_2PO_4) solutions for 3 min. After depolarization, the cells were lysed and cell proteins were separated on SDS/PAGE (66). Phosphorylated ERK1/2, RSK, and CREB were identified by immunoblotting, using the corresponding antibodies to the phosphoprotein. The net stimulation under depolarization conditions (K70) was quantified after subtracting a basal phosphorylation level at nondepolarizing conditions and normalizing with the nonphosphorylated proteins (66).

Statistics. Net phosphorylation was calculated by subtracting the basal level of phosphorylation observed in cells treated with a nondepolarizing solution (2.5K; basal) from phosphorylation triggered by depolarizing solution (70K; dep). The values shown are averages (±SEM) of triplicates carried out in three independent experiments normalized with the corresponding nonphosphorylated protein. Different mutations or selective inhibitors were compared with the WT channel. Statistical significance between two groups was evaluated with Student's *t* test, and one-way analysis of variance (ANOVA) determined statistically significant differences between the means of three

or more independent groups. Statistics were performed in GraphPad Prism 5. In the figures the criterion for statistical significance was set at $*P < 0.05$, $**P < 0.01$, and $***P < 0.005$.

ACKNOWLEDGMENTS. We thank Prof. M. Spira for assistance in confocal measurements and Dr. Eilon Sherman and Dr. Julia Sajman for PALM imaging. This work was supported by the H. L. Lauterbach Fund (D.A.).

1. Greenberg ME, Ziff EB, Greene LA (1986) Stimulation of neuronal acetylcholine receptors induces rapid gene transcription. *Science* 234:80–83.
2. Murphy TH, Worley PF, Baraban JM (1991) L-type voltage-sensitive calcium channels mediate synaptic activation of immediate early genes. *Neuron* 7:625–635.
3. Hardingham GE, Chawla S, Johnson CM, Bading H (1997) Distinct functions of nuclear and cytoplasmic calcium in the control of gene expression. *Nature* 385:260–265.
4. Bading H, Ginty DD, Greenberg ME (1993) Regulation of gene expression in hippocampal neurons by distinct calcium signaling pathways. *Science* 260:181–186.
5. Deisseroth K, Bito H, Tsien RW (1996) Signaling from synapse to nucleus: Postsynaptic CREB phosphorylation during multiple forms of hippocampal synaptic plasticity. *Neuron* 16:89–101.
6. Morgan JI, Curran T (1986) Role of ion flux in the control of c-fos expression. *Nature* 322:552–555.
7. Farnsworth CL, et al. (1995) Calcium activation of Ras mediated by neuronal exchange factor Ras-GRF. *Nature* 376:524–527.
8. Dolmetsch RE, Pajvani U, Fife K, Spotts JM, Greenberg ME (2001) Signaling to the nucleus by an L-type calcium channel-calmodulin complex through the MAP kinase pathway. *Science* 294:333–339.
9. Deisseroth K, Mermelstein PG, Xia H, Tsien RW (2003) Signaling from synapse to nucleus: The logic behind the mechanisms. *Curr Opin Neurobiol* 13:354–365.
10. Bading H, Greenberg ME (1991) Stimulation of protein tyrosine phosphorylation by NMDA receptor activation. *Science* 253:912–914.
11. Burgoyne RD (2007) Neuronal calcium sensor proteins: Generating diversity in neuronal Ca2+ signalling. *Nat Rev Neurosci* 8:182–193.
12. Wayman GA, Lee YS, Tokumitsu H, Silva AJ, Soderling TR (2008) Calmodulin-kinases: Modulators of neuronal development and plasticity. *Neuron* 59:914–931, and erratum (2009) 64:590.
13. Sheng M, McFadden G, Greenberg ME (1990) Membrane depolarization and calcium induce c-fos transcription via phosphorylation of transcription factor CREB. *Neuron* 4: 571–582.
14. Rosen LB, Ginty DD, Weber MJ, Greenberg ME (1994) Membrane depolarization and calcium influx stimulate MEK and MAP kinase via activation of Ras. *Neuron* 12: 1207–1221.
15. Rusanescu G, Qi H, Thomas SM, Brugge JS, Halegoua S (1995) Calcium influx induces neurite growth through a Src-Ras signaling cassette. *Neuron* 15:1415–1425.
16. Ma H, et al. (2014) γCaMKII shuttles Ca^{2+}/CaM to the nucleus to trigger CREB phosphorylation and gene expression. *Cell* 159:281–294.
17. Lerner I, et al. (2006) Ion interaction at the pore of Lc-type Ca2+ channel is sufficient to mediate depolarization-induced exocytosis. *J Neurochem* 97:116–127.
18. Trus M, et al. (2007) The L-type voltage-gated Ca2+ channel is the Ca2+ sensor protein of stimulus-secretion coupling in pancreatic beta cells. *Biochemistry* 46:14461–14467.
19. Marom M, Hagalili Y, Sebag A, Tzvier L, Atlas D (2010) Conformational changes induced in voltage-gated calcium channel Cav1.2 by BayK 8644 or FPL64176 modify the kinetics of secretion independently of Ca2+ influx. *J Biol Chem* 285:6996–7005.
20. Hagalili Y, Bachnoff N, Atlas D (2008) The voltage-gated Ca(2+) channel is the Ca(2+) sensor protein of secretion. *Biochemistry* 47:13822–13830.
21. Gez LS, Hagalili Y, Shainberg A, Atlas D (2012) Voltage-driven Ca(2+) binding at the L-type Ca(2+) channel triggers cardiac excitation-contraction coupling prior to Ca(2+) influx. *Biochemistry* 51:9658–9666.
22. Atlas D (2013) The voltage-gated calcium channel functions as the molecular switch of synaptic transmission. *Annu Rev Biochem* 82:607–635.
23. Atlas D (2014) Voltage-gated calcium channels function as Ca2+-activated signaling receptors. *Trends Biochem Sci* 39:45–52.
24. Wheeler DG, et al. (2012) Ca(V)1 and Ca(V)2 channels engage distinct modes of Ca(2+) signaling to control CREB-dependent gene expression. *Cell* 149:1112–1124.
25. Ma H, Cohen S, Li B, Tsien RW (2012) Exploring the dominant role of Cav1 channels in signalling to the nucleus. *Biosci Rep* 33:97–101.
26. Cohen-Kutner M, Nachmanni D, Atlas D (2010) CaV2.1 (P/Q channel) interaction with synaptic proteins is essential for depolarization-evoked release. *Channels (Austin)* 4: 266–277.
27. Atlas D (2010) Signaling role of the voltage-gated calcium channel as the molecular on/off-switch of secretion. *Cell Signal* 22:1597–1603.
28. Berrou L, Klein H, Bernatchez G, Parent L (2002) A specific tryptophan in the I-II linker is a key determinant of beta-subunit binding and modulation in Ca(V)2.3 calcium channels. *Biophys J* 83:1429–1442.
29. Hidalgo P, Gonzalez-Gutierrez G, Garcia-Olivares J, Neely A (2006) The alpha1-beta-subunit interaction that modulates calcium channel activity is reversible and requires a competent alpha-interaction domain. *J Biol Chem* 281:24104–24110.
30. Sajman J, Trus M, Atlas D, Sherman E (2017) The L-type voltage-gated calcium channel co-localizes with syntaxin 1A in nano-clusters at the plasma membrane. *Sci Rep* 7:11350.
31. Finlin BS, et al. (2006) Analysis of the complex between Ca2+ channel beta-subunit and the Rem GTPase. *J Biol Chem* 281:23557–23566.
32. Krey JF, et al. (2013) Timothy syndrome is associated with activity-dependent dendritic retraction in rodent and human neurons. *Nat Neurosci* 16:201–209.
33. Feig LA (2011) Regulation of neuronal function by Ras-GRF exchange factors. *Genes Cancer* 2:306–319.
34. Gross E, Goldberg D, Levitzki A (1992) Phosphorylation of the S. cerevisiae Cdc25 in response to glucose results in its dissociation from Ras. *Nature* 360:762–765.
35. Pragnell M, et al. (1994) Calcium channel beta-subunit binds to a conserved motif in the I-II cytoplasmic linker of the alpha 1-subunit. *Nature* 368:67–70.
36. De Waard M, Campbell KP (1995) Subunit regulation of the neuronal alpha 1A Ca2+ channel expressed in Xenopus oocytes. *J Physiol* 485:619–634.
37. Van Petegem F, Duderstadt KE, Clark KA, Wang M, Minor DL, Jr (2008) Alanine-scanning mutagenesis defines a conserved energetic hotspot in the CaValpha1 AID-CaVbeta interaction site that is critical for channel modulation. *Structure* 16:280–294.
38. Bannister RA, Beam KG (2013) Ca(V)1.1: The atypical prototypical voltage-gated Ca^{2+} channel. *Biochim Biophys Acta* 1828:1587–1597.
39. Finlin BS, et al. (2005) Regulation of L-type Ca2+ channel activity and insulin secretion by the Rem2 GTPase. *J Biol Chem* 280:41864–41871.
40. Hohaus A, et al. (2005) Structural determinants of L-type channel activation in segment IIS6 revealed by a retinal disorder. *J Biol Chem* 280:38471–38477.
41. Lansman JB, Hess P, Tsien RW (1986) Blockade of current through single calcium channels by Cd2+, Mg2+, and Ca2+. Voltage and concentration dependence of calcium entry into the pore. *J Gen Physiol* 88:321–347.
42. Hess P, Lansman JB, Tsien RW (1986) Calcium channel selectivity for divalent and monovalent cations. Voltage and concentration dependence of single channel current in ventricular heart cells. *J Gen Physiol* 88:293–319.
43. West AE, Greenberg ME (2011) Neuronal activity-regulated gene transcription in synapse development and cognitive function. *Cold Spring Harb Perspect Biol* 3: a005744.
44. Sather WA, McCleskey EW (2003) Permeation and selectivity in calcium channels. *Annu Rev Physiol* 65:133–159.
45. Ellinor PT, Yang J, Sather WA, Zhang JF, Tsien RW (1995) Ca2+ channel selectivity at a single locus for high-affinity Ca2+ interactions. *Neuron* 15:1121–1132.
46. Kim TK, et al. (2010) Widespread transcription at neuronal activity-regulated enhancers. *Nature* 465:182–187.
47. Sharma N, Gabel HW, Greenberg ME (2015) A shortcut to activity-dependent transcription. *Cell* 161:1496–1498.
48. Yang T, Colecraft HM (2013) Regulation of voltage-dependent calcium channels by RGK proteins. *Biochim Biophys Acta* 1828:1644–1654.
49. Béguin P, et al. (2001) Regulation of Ca2+ channel expression at the cell surface by the small G-protein kir/Gem. *Nature* 411:701–706.
50. Colicelli J (2004) Human RAS superfamily proteins and related GTPases. *Sci STKE* 2004: RE13.
51. Flynn R, Zamponi GW (2010) Regulation of calcium channels by RGK proteins. *Channels (Austin)* 4:434–439.
52. Soldatov NM (2015) CACNB2: An emerging pharmacological target for hypertension, heart failure, arrhythmia and mental disorders. *Curr Mol Pharmacol* 8:32–42.
53. Buraei Z, Yang J (2013) Structure and function of the β subunit of voltage-gated Ca^{2+} channels. *Biochim Biophys Acta* 1828:1530–1540.
54. Opatowsky Y, Chomsky-Hecht O, Hirsch JA (2004) Expression, purification and crystallization of a functional core of the voltage-dependent calcium channel beta subunit. *Acta Crystallogr D Biol Crystallogr* 60:1301–1303.
55. Tadmouri A, et al. (2012) Cacnb4 directly couples electrical activity to gene expression, a process defective in juvenile epilepsy. *EMBO J* 31:3730–3744.
56. Schredelseker J, et al. (2005) The beta 1a subunit is essential for the assembly of dihydropyridine-receptor arrays in skeletal muscle. *Proc Natl Acad Sci USA* 102: 17219–17224.
57. Beurg M, et al. (1999) Involvement of the carboxy-terminus region of the dihydropyridine receptor beta1a subunit in excitation-contraction coupling of skeletal muscle. *Biophys J* 77:2953–2967.
58. Schneider MF, Chandler WK (1973) Voltage dependent charge movement of skeletal muscle: A possible step in excitation-contraction coupling. *Nature* 242:244–246.
59. Rios E, Brum G (1987) Involvement of dihydropyridine receptors in excitation-contraction coupling in skeletal muscle. *Nature* 325:717–720.
60. Rebbeck RT, et al. (2011) The β(1a) subunit of the skeletal DHPR binds to skeletal RyR1 and activates the channel via its 35-residue C-terminal tail. *Biophys J* 100: 922–930.
61. Sheridan DC, Cheng W, Carbonneau L, Ahern CA, Coronado R (2004) Involvement of a heptad repeat in the carboxyl terminus of the dihydropyridine receptor beta1a subunit in the mechanism of excitation-contraction coupling in skeletal muscle. *Biophys J* 87:929–942.
62. Georgiou DK, et al. (2015) Ca2+ binding/permeation via calcium channel, CaV1.1, regulates the intracellular distribution of the fatty acid transport protein, CD36, and fatty acid metabolism. *J Biol Chem* 290:23751–23765.
63. Zhou Y, MacKinnon R (2003) The occupancy of ions in the K+ selectivity filter: Charge balance and coupling of ion binding to a protein conformational change underlie high conduction rates. *J Mol Biol* 333:965–975.
64. Lockless SW, Zhou M, MacKinnon R (2007) Structural and thermodynamic properties of selective ion binding in a K+ channel. *PLoS Biol* 5:e121.
65. Bachnoff N, Cohen-Kutner M, Trus M, Atlas D (2013) Intra-membrane signaling between the voltage-gated Ca2+-channel and cysteine residues of syntaxin 1A coordinates synchronous release. *Sci Rep* 3:1620.
66. Cohen-Kutner M, et al. (2013) Thioredoxin-mimetic peptides (TXM) reverse auranofin induced apoptosis and restore insulin secretion in insulinoma cells. *Biochem Pharmacol* 85:977–990.